A unifying Lyapunov-based approach for Time-Coordinated 3D Path-Following of multiple Quadrotors in $\mathsf{SO}(3)$

Venanzio Cichella †, Isaac Kaminer †, Enric Xargay ‡, Vladimir Dobrokhodov †,
Naira Hovakimyan ‡, Pedro Aguiar § and António M. Pascoal §

† *Naval Postgraduate School, Monterey, CA 93943.*
‡ *University of Illinois at Urbana-Champaign, Urbana, IL 61801.*
§ *Instituto Superior Técnico, Lisbon, 1049 Portugal*

***Abstract*— This paper focuses on the problem of computing control laws to solve the *Time-Coordinated 3D Path-Following* of multiple Quadrotor UAVs in the presence of time-varying communication networks and spatial and temporal contraints. In what follows, n Quadrotors are asked to track the position of n *virtual targets* moving along predifined spatial paths (parameterized by some variable $\gamma_i, \quad i = 1, ..., n$) with desired feasible speed profiles, while coordinating along the desired trajectories. One possible scenario is the situation where four vehicles are positioned in four corners of a square room. When the mission starts, every quadrotor is required to execute collision free maneuvres under strict spacial limitations, and arrive at the opposite corner at the same desired instant $t_{f,d}$. In this work, the path-following control algorithm is derived using the Special Orthogonal group theory ($\mathsf{SO}(3)$), thus avoiding complexities and singularities that arise when dealing with local parameterizations of the vehicle's attitude. The coordination task, as well as the convergence of the actual speed profile of the *virtual targets* to the desired feasible speed profile of the mission, are solved by adjusting the acceleration of the *virtual target* along the spatial paths.**

I. Introduction

Recent military conflicts, as well as surveillance and support missions, have put the global spotlight on the development of Unmanned Aerial Vehicles (UAVs). Currently, the use of UAVs plays a crucial role in preventing the exposure of human beings to uncertain environments, therefore avoiding any danger to lives. For instance, after being struck by the biggest recorded earthquake and a devastating tsunami, Japan has been fighting a potential nuclear catastrophe, deploying UAVs in situations where the presence of human operators was hazardous.

From a design point of view, and with a slight abuse of terminology, UAVs, or aircrafts in general, can be classified in two main categories: fixed-wings and rotatory-wings. Compared to fixed-wings, that do not have the potential to hold a constant position, or to move in any direction (rotate), rotorcrafts can be deployed in a much wider variety of scenarios. Among rotatory-wings aircrafts, Quadrotors play an important role in research areas as prototypes for real life applications, but also for small-area monitoring, building exploration and intervention in hostile environments.

A Quadrotor consists of two pairs of symmetrically pitched blades, whose control motion is achieved by adjusting the rotation rate of one or more rotor discs. Even though a big part of the research has been focusing on improving sensors and actuators technology and vehicle's design, many recent scientific works demonstrate the today's progress on the formulation and implementation of new control algorithms for the motion control of the Quadrotors. To mention a few, [1] and [2] use the Lyapunov stability theory for the stabilization and control of the vehicle. In [3] and [4] conventional PD^2 feedback and PID structures are used for simpler implementation of the control laws, and are compared with LQR based optimal control theory. Backstepping control is proposed in [5], while in [6] and [7] a visual feedback control law is presented using offboard or onboard cameras for pose estimation. Fuzzy logic control techniques are proposed in [8]. Intelligent control, based on neural networks, is introduced in [9] to achieve vertical take off and landing. Finally, integral sliding mode and reinforcement learning control are presented in [10] as solutions for accomodating the nonlinear disturbances for outdoor altitude control. The path-following control law presented in this paper refers to the work introduced in [11], where a Lyapunov based control is formulated using the Special Orthogonal group ($\mathsf{SO}(3)$) theory, leading to a simple and singularity free solution for the trajectory tracking problem. A similar idea has already been adopted by the author in [12], where a solution for the 3D path-following problem for fixed-wings UAVs was presented. Moreover, motivated by more challenging scenarios, the same algorithm was employed in [13], where multiple fixed-wings UAVs were asked to coordinate while following their desired paths.

The use of multiple vehicles working in cooperation to achieve a common objective has captured the attention of control community in recent years. Relevant works developed in this area include spacecraft formation flying [14], UAV control [15], [16], coordinated control of land robots [17], and control of multiple autonomous underwater vehicles [18], [19]. In spite of significant progress in the field, much work remains to be done to develop strategies capable

Research supported in part by projects USSOCOM, ONR under Contract N00014-11-WX20047, ONR under Contract N00014-05-1-0828, AFOSR under Contract No. FA9550-05-1-0157, ARO under Contract No. W911NF-06-1-0330, and CO3AUVs of the EU (Grant agreement n. 231378)

of yielding robust performance of a fleet of vehicles in presence of critical constraints. For example, as pointed out in [20], [21], one of the crucial problems is the presence of time-varying communication networks due to temporary loss of communication links and switching communication topologies.

Motivated by these and similar challenges, in this paper we address the problem of steering a fleet of Quadrotor UAVs along desired paths while meeting stringent spatial and temporal constraints. A typical example is the situation where a set of vehicles must break up and arrive at assigned targets in the same time. The solution proposed unfolds in two basic steps: first, a path-following control law is designed to position each vehicle on a *virtual target* (VT) moving along a predefined spatial path; in the second step, the accelerations of the VTs are adjusted so as to synchronize their positions according to a desired time law to achieve, indirectly, vehicle coordination.

This paper is organized as follows. Section II defines the 3D Path-Following (PF) problem for a single Quadrotor UAV, while III furmulates the Time-Coordination (TC) problem for a fleet of vechiles. In Section IV the two problems described in the aforementioned Sections are combined, giving a definition of Time-Coordinated 3D Path-Following (TCPF). Section V addresses the stability and convergence properties of the TCPF problem. Section VI presents simulation results. Finally, Section VII summarizes the key results and contains the main conclusions.

II. 3D Path-Following

In this Section the PF problem for a single Quadrotor UAV is described as follows. First, we consider the kinematic and dynamic of the system, without considering the dynamic of the rotor and the propellers, and the moments acting on the rigid body. Second, we consider limited performance of an onboard autopilot tracking commanded total thrust and angular velocities.

A. Problem Formulation

Let $\mathcal{I} = [\vec{e}_1^\top, \vec{e}_2^\top, \vec{e}_3^\top]^\top$ and $\mathcal{B} = [\vec{b}_1^\top, \vec{b}_2^\top, \vec{b}_3^\top]^\top$ be two coordinate frames representing, respectively, the inertial frame and the body frame attached to the Quadrotor. Let $x_d(\gamma)$ be a desired path parameterized by some variable γ, and let us call "virtual target" (VT) a moving point along the predifined desired path. The choice of the parameter γ is discussed later.

Let the motion of the Quadrotor be governed by

$$\begin{cases} \dot{x} = v \\ m\dot{v} = f\vec{b}_3 - mg\vec{e}_3 \\ \dot{R} = RS(\omega)\,, \end{cases} \tag{1}$$

where $x(t)$ and $v(t)$ are the position and velocity of the Quadrotor, m is its mass, $f(t)$ is the total thrust of the four propellers, $R = R_B^I$ the rotation matrix from the body frame to the inertial frame, and $\omega = [p(t), q(t), r(t)]$ the angular velocity of the vehicle expressed in $\mathcal{B}$. Then, we can define the position error vector $e_x \in \mathbb{R}^3$ as

$$e_x(t) = x_d(\gamma) - x(t) \tag{2}$$

and the velocity error vector $e_v \in \mathbb{R}^3$ as

$$e_v(t) = \frac{\partial x_d(\gamma)}{\partial \gamma} - \dot{x}(t)\,. \tag{3}$$

Assume, without loss of generality, that the desired velocity and acceleration are bounded, that is:

$$\left|\left|\frac{\partial x_d}{\partial \gamma}\right|\right| \leq b_1 \tag{4}$$

$$\left|\left|\frac{\partial^2 x_d}{\partial \gamma^2}\right|\right| \leq b_2 \tag{5}$$

for some $b_1, b_2 > 0$.

Let $\mathcal{D}$ be the frame representing the desired attitude to shape the approach to the path. Let the rotation matrix from the frame $\mathcal{D}$ to the inertial frame $\mathcal{I}$ be [11]:

$$R_D^I = R_c = [\vec{b}_{1D}, \vec{b}_{3D} \times \vec{b}_{1D}, \vec{b}_{3D}]$$

where

$$\vec{b}_{3D} = \frac{k_x e_x + k_v e_v + mg\vec{e}_3 + m\frac{\partial^2 x_d}{\partial \gamma^2}}{||k_x e_x + k_v e_v + mg\vec{e}_3 + m\frac{\partial^2 x_d}{\partial \gamma^2}||} \tag{6}$$

and $\vec{b}_{1D}$ is chosen in order to be orthonormal to $\vec{b}_{3D}$. Assume

$$||k_x e_x + k_v e_v + mg\vec{e}_3 + m\frac{\partial^2 x_d}{\partial \gamma^2}|| \neq 0 \tag{7}$$

and

$$||mg\vec{e}_3 + m\frac{\partial^2 x_d}{\partial \gamma^2}|| < B\,. \tag{8}$$

Let $\tilde{R}$ be the rotation matrix from $\mathcal{B}$ to $\mathcal{D}$, that is

$$\tilde{R} = R_B^D = R_c^\top R\,.$$

Then,

$$\dot{\tilde{R}} = \tilde{R}S(\tilde{\omega})$$

where

$$\tilde{\omega} = \omega_{BD}^B = \begin{bmatrix} p \\ q \\ r \end{bmatrix} - \tilde{R}^\top \omega_{DI}^D\,, \tag{9}$$

and

$$S(\omega_{DI}^D) = R_c^\top \dot{R}_c\,.$$

The objective is then to drive the position error e_x and the velocity error e_v to zero, and the rotation matrix $\tilde{R}$ to the identity.
Consider the real-valued function on SO(3) [11]:

$$\Psi(\tilde{R}) = \frac{1}{2} tr(I - \tilde{R})\,, \tag{10}$$

and its time derivative

$$\dot{\Psi}(\tilde{R}) = -\frac{1}{2} tr(\tilde{R}S(\tilde{\omega})).$$

Finally, let the attitude error vector be [11]

$$e_{\tilde{R}} = \sqrt{\Psi(\tilde{R})(2-\Psi(\tilde{R}))}\,\frac{1}{2}vec(\tilde{R}-\tilde{R}^{\top})\,. \tag{11}$$

Using properties of the $SO(n)$ group [22], we get:

$$\dot{\Psi}(\tilde{R}) = \frac{1}{2}e_{\tilde{R}}\cdot\tilde{\omega}\,. \tag{12}$$

Then, the dynamic of the path-following error can be summarized in the following system of equations:

$$\begin{cases} \dot{e}_x = \frac{\partial x_d}{\partial \gamma}\dot{\gamma} - \dot{x} \\ m\dot{e}_v = m\frac{\partial^2 x_d}{\partial \gamma^2}\dot{\gamma} - f\vec{b}_3 + mg\vec{e}_3 \\ \dot{\Psi}(\tilde{R}) = \frac{1}{2}e_{\tilde{R}}\cdot\tilde{\omega}\,. \end{cases} \tag{13}$$

Using the above notation, we now define the problem of *path-following* for a single vehicle.

Definition 1: **Path-Following Problem (PF):** For a given Quadrotor UAV, and for a given spatially defined path $p_d(\gamma)$, design feedback control laws for the total thrust of the four propellers $f(t)$, the roll rate $p(t)$, pitch rate $q(t)$ and yaw rate $r(t)$ such that the generalized path-following error vector $x_{PF} = [e_x\,,\, e_v\,,\, e_{\tilde{R}}]$, with the dynamic described in (13), converges to a neighborhood of the origin, for any physically feasible temporal speed assignment of the mission.

B. Quadrotor with autopilot

As discussed in Definition 1, one of the purpose of the paper is to drive the position, velocty and attitude error vectors to a neighborhood of the origin, using the total thrust of the four propellers and the angular velocities of the vehicle. The vehicles at hand are equipped with an onboard autopilot (AP), in charge of tracking the thrust and angular velocity references. For that reason, it is fair to take into account possible limits on the performance of the AP. Therefore, we assume that :

$$|p_c(t) - p(t)| \leq \delta_p \tag{14}$$

$$|q_c(t) - q(t)| \leq \delta_q \tag{15}$$

$$|r_c(t) - r(t)| \leq \delta_r \tag{16}$$

$$|f_c(t) - f(t)| \leq \delta_f \tag{17}$$

where $p_c(t)\,,\, q_c(t)\,,\, r_c(t)\,,\, f_c(t)$ are the commanded inputs from the controller to the AP, $p(t)\,,\, q(t)\,,\, r(t)\,,\, f(t)$ are the actual commanded values from the inner loop architecture to the vehicle, and $\delta_p, \delta_q, \delta_r, \delta_f$ are the bounds which characterize the tracking performance of the AP.

III. Time-Coordination of a fleet of Quadrotor UAVs: Problem Formulation

We now address the problem of the time coordination of a fleet of n Quadrotor UAVs.

As described in the Section II, the desired path of every vehicle is parameterized by some variable γ_i, with $i = 1\,,\,\ldots\,,\,n$. The choice of the parameter γ_i is such that, if $\gamma_i - \gamma_j = 0$, then the i-th and j-th UAVs are synchronized.

In order to coordinate, the synchronization states have to be exchanged among the Quadrotors over a communication network. Using tools from graph theory we model the information exchanged over the time-varying network as well as the constraints imposed by the communication topology. We start assuming that the i-th UAV communicates only with a neighboring set of vehicles, denoted by $\mathcal{G}_i$. We also assume that the communication between two UAVs is bidirectional with no delays.

We now let $L(t) \in \mathbb{R}^{n\times n}$ be the Laplacian of the graph $\Gamma(t)$. Let $Q \in \mathbb{R}^{(n-1)\times n}$ be a matrix such that $Q\mathbf{1}_n = 0$, $QQ^{\top} = I_{n-1}$ and $\bar{L}(t) = QL(t)Q^{\top}$, where $\bar{L} \in \mathbb{R}^{(n-1)\times(n-1)}$ with the spectrum equal to the spectrum of $L(t)$ without the eigenvalue $\lambda_1 = 0$. Finally, we let $\bar{L}(t)$ satisfy the persistency of excitation assumption:

$$\int_{t}^{t+T} \bar{L}(\tau)d\tau = \mu I_{n-1}\,. \tag{18}$$

Given the above notation, we now let

$$\xi(t) = Q\gamma(t) \tag{19}$$

where $\xi(t) = [\xi_1(t), \xi_2(t), ..., \xi_{n-1}(t)] \in \mathbb{R}^{n-1}$ and $\gamma(t) = [\gamma_1(t), \gamma_2(t), ..., \gamma_n(t)] \in \mathbb{R}^n$. From the definition of Q, if $\xi(t) = \mathbf{0}^n$, then $\gamma_i - \gamma_j = 0 \quad \forall\, i, j = 1\,,\,\ldots\,,\,n$.

Let also

$$z(t) = \dot{\gamma}(t) - 1\,, \tag{20}$$

where $z(t) = [z_1(t), z_2(t), ..., z_n(t)] \in \mathbb{R}^n$. Note that, if $z_i = 0$, then the progression of the i-th VT converges to the time progression. In other words, if $z_i = 0$, then $\gamma_i \to t$.

With the above notation, the coordination problem can be defined.

Definition 2: **Time Coordination Problem (TC):** Given a set of n 3D desired trajectories $p_{di}(\gamma_i)$, design feedback control law for $\ddot{\gamma}_i = \dot{z}_i$ such that the vectors ξ and z defined, respectively, in (19) and (20), converge exponentially to a neighborhood of the origin $\forall\, i = 1\,,\,\ldots\,,\,n$.

IV. Time-Coordinated 3D Path-Following: Problem Formulation

In the previous sections we formulated the PF problem for a single vehicle, and the TC problem for a fleet of n Quadrotor UAVs. In this section we summarize this two problems into a single one, by giving a definition of Time Coordinated 3D Path Following. Let us assume, without loss of generality, that $m_i = m_j \quad \forall\, i, j = 1\,,\,\ldots\,,\,n$. Consider the

dynamic of the path following error variables in (13). Using the variable z defined in (20), we get

$$\begin{cases} \dot{e}_{xi} = \frac{\partial x_{di}}{\partial \gamma_i} z_i + e_{vi} \\ m\dot{e}_{vi} = m\frac{\partial^2 x_{di}}{\partial \gamma_i^2} z_i + m\frac{\partial^2 x_{di}}{\partial \gamma_i^2} - f\vec{b}_{3i} + mg\vec{e}_3 \\ \dot{\Psi}(\tilde{R}_i) = \frac{1}{2} e_{\tilde{R}i} \cdot \tilde{\omega}_i \,. \end{cases} \tag{21}$$

$\forall\, i = 1\,,\, \ldots\,,\, n.$

Let $e_x\,,\, e_v\,,\, e_{\tilde{R}}$ and $\Psi(\tilde{R})$ be

$$e_x = [e_{x1}^\top\,,\, e_{x2}^\top\,,\, \ldots\,,\, e_{xn}^\top]^\top \in \mathbb{R}^{3n\times 1}\,, \tag{22}$$

$$e_v = [e_{v1}^\top\,,\, e_{v2}^\top\,,\, \ldots\,,\, e_{vn}^\top]^\top \in \mathbb{R}^{3n\times 1}\,, \tag{23}$$

$$e_{\tilde{R}} = [e_{\tilde{R}1}^\top\,,\, e_{\tilde{R}2}^\top\,,\, \ldots\,,\, e_{\tilde{R}n}^\top]^\top \in \mathbb{R}^{3n\times 1}\,, \tag{24}$$

and

$$\Psi(\tilde{R}) = \sum_{i=1}^{n} \Psi(\tilde{R}_i) \in \mathbb{R}\,, \tag{25}$$

and let $x_{PF} = [e_x^\top\,,\, e_v^\top\,,\, e_{\tilde{R}}^\top]^\top$. Recall also the TC error variables defined in (19) and (20). Then, the objective of this paper can be stated as follows:

Definition 3: **Time Coordinated 3D Path Following (TCPF):** Given a fleet of n UAVs, a communication network satisfying (18) and a set of n 3D desired trajectories $p_{di}(\gamma_i)$, design feedback control laws for the total thrust $f_i(t)$ and for roll rate $p_i(t)$, pitch rate $q_i(t)$ and yaw rate $r_i(t)$ such that the PF errors, with the dynamic described in (21) , converge to a neighborhood of the origin $\forall\, i = 1\,,\, \ldots\,,\, n$. Also, design a feedback control law for $\ddot{\gamma}_i = z_i$ such that the TC errors defined in (19) and (20) converge to zero.

V. Time-Coordinated 3D Path-Following: Main Result

First, let the total thrust of the i-th vehicle be governed by

$$f_i = \left(k_x e_{xi} + k_v e_{vi} + mge_3 + m\frac{\partial^2 x_{di}}{\partial \gamma_i^2}\right)^\top \vec{b}_{3i}\,. \tag{26}$$

In addition, let the angular rates of the i-th quadrotor be

$$\begin{bmatrix} p_i \\ q_i \\ r_i \end{bmatrix} = \tilde{R}_i^\top \omega_{D_i I}^{D_i} - 2k_{\tilde{R}} e_{\tilde{R}i}. \tag{27}$$

Finally, let

$$\ddot{\gamma} = \dot{z} = -bz - aL\gamma. \tag{28}$$

In the Lemma below is stated one of the main results of this work:

Lemma 1: **TCPF with ideal inner-loop tracking performance:**

Let $k_x\,, k_v\,, k_{\tilde{R}}\,, c_1\,, a$ and b be positive constants that satisfy inequalities (29), (30) and (31).

$$\begin{bmatrix} \frac{k_x}{2} & \frac{c_1}{2} & 0 \\ \frac{c_1}{2} & \frac{m}{2} & 0 \\ 0 & 0 & \frac{1}{2} \end{bmatrix} > 0 \tag{29}$$

Then, the control inputs in (26), (27) and (28) ensure that the error vector

$$x = [e_x^\top\,,\, e_v^\top\,,\, e_{\tilde{R}}^\top\,,\, \xi^\top\,,\, z^\top]^\top$$

converge exponentially to *zero* with rate of convergence

$$\lambda \triangleq \min(\lambda_{PF}\,,\, \lambda_{TC})\,, \tag{32}$$

for any

$$\lambda_{PF} > 0 \tag{33}$$

and with

$$\lambda_{TC} < \frac{\mu}{T(1+n^2T)^2} \tag{34}$$

and corresponding domain of attraction

$$\Omega_c \triangleq \left\{(e_x\,, e_{\tilde{R}}) \;\mid\; \Psi(\tilde{R}) \le c^2 < 1\,, ||e_x|| \le e_{x\,\max}\right\}. \tag{35}$$

A proof of this result is given in the Appendix.

Remark 1: Constants k_x, k_v, $k_{\tilde{R}}$, c_1, a and b that satisfy inequalities (29), (30) and (31) are derived in the Appendix.

As our last step, we consider the case of non perfect inner-loop tracking discussed in Section II-B. The main result of our work follows.

Lemma 2: **TCPF with non perfect inner-loop tracking performance:** Let $k_x\,, k_v\,, k_{\tilde{R}}\,, c_1\,, a$ and b be positive constants that satisfy the inequalities (29), (30), (31) and

$$k_x > \frac{4c_1^2}{m\epsilon_x\epsilon_v}\,.$$

Let the control inputs be governed by (26), (27) and (28). Let θ be a positive constant such that

$$0 < \theta < \lambda\,, \tag{36}$$

where λ was defined in (32). Let also the performance bounds defined in Section II-B, satisfy

$$\gamma_f < \frac{e_{x\,\max} k_x m\theta}{2c_1}\,, \tag{37}$$

and

$$\gamma_\omega \triangleq \sqrt{\gamma_p^2 + \gamma_r^2 + \gamma_r^2} < \frac{c\theta}{2-c^2}\,. \tag{38}$$

Then, for any initial state $x(0) = [e_x(0)^\top\,, e_v(0)^\top\,, e_{\tilde{R}}(0)^\top\,, \xi(0)^\top\,, z(0)^\top]^\top \in \Omega_c$ there is a time $T_b \ge 0$ such that the bound in (39) holds $\forall\; 0 \le t < T_b$, and the bound in (40) holds $\forall\; t \ge T_b$.

The proof of this result is given in the Appendix.

Remark 2: Note that the limits on the performance of the autopilot affect only the convergence of the PF errors $x_{PF} = [e_x^\top\,, e_v^\top\,, e_{\tilde{R}}^\top]^\top$. In fact, it can be stated that, $\forall\, t \ge 0$,

$$\begin{aligned} &\left(\frac{b^2\bar{c}_3}{2n}||\xi(t)||^2 + \frac{b\bar{c}_3}{n}\xi(t)^\top z(t) + \right. \\ &\left. + \frac{1}{2}\left(\frac{\bar{c}_3}{n} + 1\right)||z(t)||^2\right) \le \left(\frac{b^2\bar{c}_4}{2\gamma_\lambda}||\xi(0)||^2 + \right. \\ &\left. + \frac{b\bar{c}_4}{\gamma_\lambda}\xi(0)^\top z(0) + \frac{1}{2}\left(\frac{\bar{c}_4}{\gamma_\lambda} + 1\right)||z(0)||^2\right) e^{-\lambda_{TC}t}\,. \end{aligned} \tag{41}$$

This consideration is discussed in details in the Appendix.

$$\begin{bmatrix} \left(k_x\left(\frac{c_1}{m}(1-c^2)-b_1\right)-c_1b_2\right)-\frac{k_x}{2}\lambda_{PF} & -\frac{c_1k_v}{m}(1+c^2)-\frac{c_1}{2}\lambda_{PF} & -\frac{B_ic_1}{m} \\ -\frac{c_1k_v}{m}(1+c^2)-\frac{c_1}{2}\lambda_{PF} & (k_v(1-c^2)-c_1-c_1b_1-mb_2)-\frac{m}{2}\lambda_{PF} & -(k_xe_{x\max}+B) \\ -\frac{B_ic_1}{m} & -(k_xe_{x\max i}+B) & k_{\tilde{R}}-\frac{1}{2-c^2}\lambda_{PF} \end{bmatrix} \geq 0 \quad (30)$$

$$\begin{bmatrix} \bar{c}_3-\frac{\bar{c}_4}{2\gamma_\lambda}\lambda_{TC} & -n\left(\frac{\bar{c}_4}{\gamma_\lambda}+1\right) \\ -n\left(\frac{\bar{c}_4}{\gamma_\lambda}+1\right) & (b-n-(k_x+c_1)b_1-(c_1+m)b_2-\frac{\lambda_{TC}}{2}) \end{bmatrix} \geq 0 \quad (31)$$

$$\frac{k_x}{2}||e_x(t)||^2+\frac{m}{2}||e_v(t)||^2+\Psi(\tilde{R}(t))+c_1(e_v(t)^\top e_x(t))+\frac{b^2\bar{c}_3}{2n}||\xi(t)||^2+\frac{b\bar{c}_3}{n}\xi(t)^\top z(t)+\frac{1}{2}\left(\frac{\bar{c}_3}{n}+1\right)||z(t)||^2$$
$$\leq\left(\frac{k_x}{2}||e_x(0)||^2+\frac{m}{2}||e_v(0)||^2+\Psi(\tilde{R}(0))+c_1(e_v(0)^\top e_x(0))+\frac{b^2\bar{c}_4}{2\gamma_\lambda}||\xi(0)||^2+\frac{b\bar{c}_4}{\gamma_\lambda}\xi(0)^\top z(0)+\frac{1}{2}\left(\frac{\bar{c}_4}{\gamma_\lambda}+1\right)||z(0)||^2\right)e^{-(\lambda-\theta)t} \quad (39)$$

$$||e_x||\leq\frac{2c_1\delta_f}{k_xm\theta(1-\epsilon_x)}\,,\ ||e_v||\leq\frac{2\delta_f}{m\theta(1-\epsilon_v)}\,,\ ||e_{\tilde{R}}||\leq\frac{2-c^2}{2}\frac{\delta_\omega}{\theta} \quad (40)$$

VI. Simulation Results

In this Section, simulation results are presented. The scenario at hand involves four vehicles. The UAVs are asked to follow four intersecting paths. The geometry of the given paths, and the constant desired speed profiles, ensure collision avoidance. Figure 1 illustrates the mission at hand. The initial value for the vector $\dot{\gamma}$ has been initialized away from the desired value. More precisely, has illustrated in Figure 2, $\dot{\gamma}_i(0) \quad i=1,...,4$ as been chosen as follow:

$$\dot{\gamma}_1(0)=1.5\,,$$
$$\dot{\gamma}_2(0)=0.5\,,$$
$$\dot{\gamma}_3(0)=2\,,$$
$$\dot{\gamma}_4(0)=0\,.$$

This initialization leads to an initial error in the coordination variable. However, the control algorithm ensures the convergence to the origin of the coordination state.

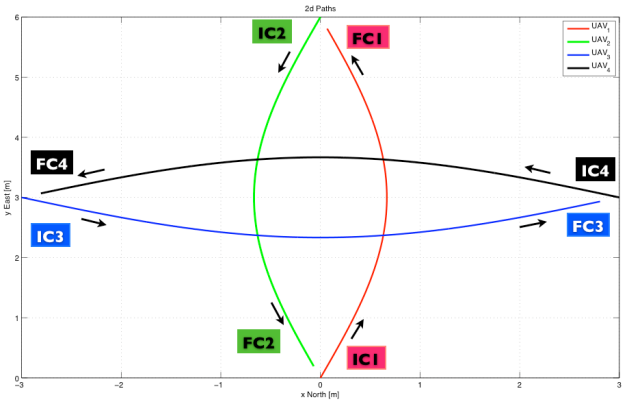

Fig. 1

VII. Conclusion

In this paper we considered the problem of steering a fleet of Quadrotor Unmanned Aerial Vehicles (UAVs) along predefined spatial paths, while coordinating with each others, accordingly to the mission requirements. Cooperative control is achieved in presence of time-varying communication networks, and stringent spatial and temporal contraints. The constraints include collision-free maneuver and simultaneus times of arrival at desired locations, accordingly to the desired speed profile of the mission. The Path-Following problem, which lies in tracking the position of a *virtual target* along its spatial path, is solved using the Special Orthogonal group theory, which avoids the complexities and singularities that arise using local parameterization of the vehicle's attitude. Angular velocities and total thust are used to drive the Quadrotors in the desired positions. For that reason, is assumed that the vehicles are equipped with commercial autopilots. Hence, non-ideal inner-loop tracking performance are also considered. Coordination between the UAVs is achieved adjusting the acceleration of the *virtual targets* along the desired trajectories. Exponential convergence of the Time-Coordinated 3D Path-Following errors is guaranteed and demonstrated using Lyapunov theory.

References

[1] P. Murrieri S. Bouabdallah and R. Siegwart. Design and control of an indoor micro quadrotor. In *Proc. of The International Conference on Robotics and Automation (ICRA)*, 2004.

[2] P. Castillo A. Dzul and L. Lozano. Real-time stabilization and tracking of a four rotor mini rotorcraft. In *IEEE Transaction on Control System Technology*, volume 12(4), pages 510–516, 2004.

[3] A. Tayebi and S. McGilvray. Attitude stabilization of a vtol quadrotor aircraft. In *IEEE Transaction on Control System Technology*, volume 14(3), pages 562–571, May 2006.

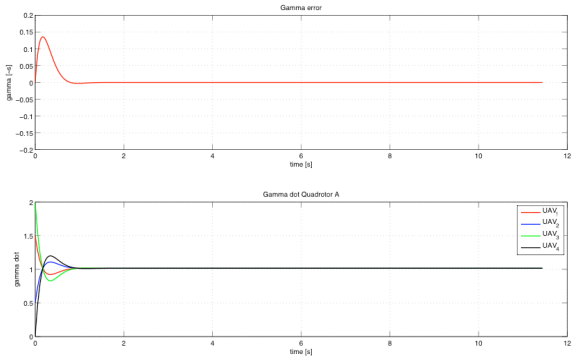

Fig. 2

[4] A. Noth S. Bouabdallah and R. Siegwart. Pid vs lqr control techniques applied to an indoor micro quadrotor. In *International Conference on Intelligent Robots and Systems*, 2004.

[5] T. Hamel N. Guenard and V. Moreau. Dynamic modeling and intuitive control strategy for an x4-flyer. In *International Conference on Robotics and Automation (ICRA)*, pages 141–146, 2005.

[6] J.P. Ostrowski E. Altug and R. Mahony. Control of a quadrotor helicopter using visual feedback. In *Proc. of the 2002 IEEE International Conference on Robotics and Automation (ICRA)*, pages 72–77, 2002.

[7] T. Hamel N. Guenard and R. Mahony. A practical visual servo control for an unmanned aerial vehicle. In *IEEE Transaction on Robotics*, volume 24(2), pages 331–340, 2008.

[8] C. Coza and C.J.B Macnab. A new robust adaptive-fuzzy control method applied to quadrotor helicopter stabilization. In *Annual meeting of the North American Fuzzy Information Processing Society*, pages 454–458, 2006.

[9] J. Dunfied M. Tarbouchi and G. Labonte. Neural network based control of a four rotor helicopter. In *International Conference on Industrial Technology*, pages 1543–1548, 2004.

[10] J.S. Jang S.L. Waslander, G.M. Hoffman and C.J. Tomlin. Multi-agent quadrotor testbed control design: integral sliding mode vs reinforcement learning. In *International Conference on Intelligent Robots and Systems*, pages 468–473, 2005.

[11] Taeyoung Lee, Melvin Leok, and N. Harris McClamroch. Control of complex maneuvers for a quadrotor UAV using geometric methods on $\mathsf{SE}(3)$. *IEEE Transactions on Automatic Control*, 2010. Submitted. Available online: `arXiv:1003.2005v3`.

[12] Vladimir Dobrokhodov Enric Xargay Naira Hovakimyan Venanzio Cichella, Isaac Kaminer and Antonio Pascoal. Geometric 3d path-following control for a fixed-wing uav on $\mathsf{SO}(3)$. In *AIAA Guidance, Navigation and Control Conference*, Portland, Oregon, August 2011. AIAA-2011-6415.

[13] Enric Xargay, Isaac Kaminer, António M. Pascoal, Naira Hovakimyan, Vladimir Dobrokhodov, Venanzio Cichella, A. Pedro Aguiar, and Reza Ghabcheloo. Time-critical cooperative path following of multiple UAVs over time-varying networks. Submitted to *IEEE Transactions on Control System Thechnology*, 2011.

[14] Mehran Mesbahi and Fred Y. Hadaegh. Formation flying control of multiple spacecraft via graphs, matrix inequalities, and switching. *Journal of Guidance, Control and Dynamics*, 24(2):369–377, March–April 2001.

[15] Yongduan D. Song, Yao Li, and Xiao H. Liao. Orthogonal transformation based robust adaptive close formation control of multi-UAVs. In *American Control Conference*, volume 5, pages 2983–2988, Portland, OR, June 2005.

[16] Dušan M. Stipanović, Gökhan İnalhan, Rodney Teo, and Claire J. Tomlin. Decentralized overlapping control of a formation of unmanned aerial vehicles. *Automatica*, 40(8):1285–1296, August 2004.

[17] Reza Ghabcheloo, António M. Pascoal, Carlos Silvestre, and Isaac Kaminer. Coordinated path following control of multiple wheeled robots using linearization techniques. *International Journal of Systems Science*, 37(6):399–414, May 2006.

[18] Reza Ghabcheloo, A. Pedro Aguiar, António M. Pascoal, Carlos Silvestre, Isaac Kaminer, and João P. Hespanha. Coordinated path-following control of multiple underactuated autonomous vehicles in presence of communication failures. In *IEEE Conference on Decision and Control*, pages 4345–4350, San Diego, CA, December 2006.

[19] F. Lobo Pereira and J. Borges de Sousa. Coordinated control of networked vehicles: An autonomous underwater system. *Automation and Remote Control*, 65(7):1037–1045, July 2004.

[20] Isaac Kaminer, António M. Pascoal, Eric Hallberg, and Carlos Silvestreo. Trajectory tracking for autonomous vehicles: An integrated approach to guidance and control. *Journal of Guidance, Control and Dynamics*, 21(1):29–38, January–February 1998.

[21] Yoonsoo Kim and Mehran Mesbahi. On maximizing the second smallest eigenvalue of state-dependent graph Laplacian. *IEEE Transactions on Automatic Control*, 51(1):116–120, January 2006.

[22] Taeyoung Lee. Robust adaptive geometric tracking controls on so(3) with an application to the attitude dynamicsof a quadrotor uav. 2011. Available: http://arxiv.org/abs/1108.6031.

[23] Antonio Loría and Elena Panteley. Uniform exponential stability of linear time-varying systems: Revisited. *Systems & Control Letters*, 47(1):13–24, September 2002.

[24] Hassan K. Khalil. *Nonlinear Systems*. Prentice Hall, Englewood Cliffs, NJ, 2002.

APPENDIX

Proof of Lemma 1 First, consider the system

$$\dot{\phi}(t) = -\bar{L}\phi(t)\,. \tag{42}$$

If we let $D(t)$ be the time-varying incidence matrix, that is $L(t) = D(t)D(t)^\top$, we can rewrite (42) as:

$$\dot{\phi}(t) = -(QD(t))(QD(t))^\top\phi(t)\,,$$

where the matrix $QD(t)$ is piecewise-constant and bounded as follow:

$$||QD(t)|| \leq n\,.$$

Therefore, since $\bar{L}$ satisfies the PE condition in (18), we can use the result in [23] (Lemma 5) to conclude that the system in (42) is GUES (global uniformally exponentially stable), and that the following bound holds:

$$||\phi(t)|| \leq k_\lambda||\phi(0)||e^{-\gamma_\lambda t}\,,$$

with

$$k_\lambda = 1\,,\quad \gamma_\lambda \geq \bar{\gamma}_\lambda \triangleq \frac{\mu}{T(1+n^2T)^2}\,.$$

Since the system in (42) is GUES, Lemma 1 in [23] and a similar argument in Theorem 4.12 [24] imply that, for any $\bar{c}_3$ and $\bar{c}_4$ satisfying $0 < \bar{c}_3 \leq \bar{c}_4$, there exist a continuously differentiable, symmetric, positive definite matrix $P_c(t)$, that is

$$0 < \bar{c}_1 \triangleq \frac{\bar{c}_3}{2n}I \leq P_c(t) \leq \frac{\bar{c}_4}{2\gamma_\lambda}I \triangleq \bar{c}_2\,, \tag{43}$$

which satisfies the matrix differential equation

$$\dot{P}_c - \bar{L}P_c - P_c\bar{L} \leq -\bar{c}_3 I\,. \tag{44}$$

Secondly, for the path following state vectors, we note that in Ω_c the following bounds hold [11] [22]:

$$\Psi(\tilde{R}_i) \leq c^2 < 1\,, \tag{45}$$

$$\frac{1}{2}||e_{\tilde{R}i}||^2 \leq \Psi(\tilde{R}_i) \leq \frac{1}{2-c^2}||e_{\tilde{R}i}||^2\,, \tag{46}$$

$$||e_{xi}|| \leq e_{x\max}\,. \tag{47}$$

Then, we note that if (45) is verified, the following inequality holds:

$$||e_{\tilde{R}i}|| \leq c^2\,. \tag{48}$$

Let us now introduce an other variable:

$$\chi(t) = b\xi(t) + Qz(t), \tag{49}$$

where $\chi(t) = [\chi_1(t), \chi_2(t), ..., \chi_{n-1}(t)]$. By driving the variable $\chi(t)$ and $z(t)$ to $zero$ we achieve time coordination. Therefore we can use the following system for the time coordination error:

$$\begin{cases} \chi = b\xi + Qz \\ z = \dot{\gamma} - 1\,. \end{cases} \tag{50}$$

Choosing the control law defined in (28), straighforward computations lead to:

$$\begin{cases} \dot{\chi} = -\frac{a}{b}\bar{L}\chi + \frac{a}{b}QLz \\ \dot{z} = -(bI - \frac{a}{b}L)z - \frac{a}{b}LQ^\top\chi\,, \end{cases} \tag{51}$$

which describes the dynamic of the time coordination error variables.

Let us choose the following Lyapunov candidate function:

$$V = \frac{k_x}{2}||e_x||^2 + \frac{m}{2}||e_v||^2 + \Psi(\tilde{R}) + c_1(e_v^\top e_x) + \chi^\top P_c\chi + \frac{1}{2}||z||^2\,, \tag{52}$$

where $c_1, k_x, m > 0$, and P_c was defined earlier. Note that (52) can be also written as:

$$V = \frac{k_x}{2}\sum_{i=1}^{n}||e_{xi}||^2 + \frac{m}{2}\sum_{i=1}^{n}||e_{vi}||^2 + \sum_{i=1}^{n}\Psi(\tilde{R}_i) + \\ + c_1\sum_{i=1}^{n}(e_{vi}^\top e_{xi}) + \chi^\top P_c\chi + \frac{1}{2}||z||^2\,.$$

The bound in (46), together with the bound in (43), allows us to write the Lyapunov candidate function as follow:

$$x_{PF}^\top W_{11}x_{PF} + x_{TC}^\top W_{21}x_{TC} \leq \\ V(x_{PF}, x_{TC}) \leq x_{PF}^\top W_{12}x_{PF} + x_{TC}^\top W_{22}x_{TC}$$

where:

$$x_{PF} = [e_x^\top(t), e_v^\top(t), e_{\tilde{R}}^\top(t)]^\top\,,$$
$$x_{TC} = [\chi^\top(t), z^\top(t)]^\top\,.$$

and

$$W_{11} = \begin{bmatrix} \frac{k_x}{2} & \frac{c_1}{2} & 0 \\ \frac{c_1}{2} & \frac{m}{2} & 0 \\ 0 & 0 & \frac{1}{2} \end{bmatrix}\,,$$

$$W_{12} = \begin{bmatrix} \frac{k_x}{2} & \frac{c_1}{2} & 0 \\ \frac{c_1}{2} & \frac{m}{2} & 0 \\ 0 & 0 & \frac{1}{2-\psi} \end{bmatrix}\,,$$

$$W_{21} = \begin{bmatrix} \frac{\bar{c}_3}{2n} & 0 \\ 0 & \frac{1}{2} \end{bmatrix}\,,$$

and

$$W_{22} = \begin{bmatrix} \frac{\bar{c}_4}{2\gamma_\chi} & 0 \\ 0 & \frac{1}{2} \end{bmatrix}\,.$$

Now, for simplicity of the proof, let us consider the Lyapunov function as the sum of two functions, that is:

$$V = \underbrace{\frac{k_x}{2}\sum_{i=1}^{n}||e_{xi}||^2 + \frac{m}{2}\sum_{i=1}^{n}||e_{vi}||^2 + \sum_{i=1}^{n}\Psi(\tilde{R}_i) + c_1\sum_{i=1}^{n}(e_{vi}^\top e_{xi})}_{V_{PF}} + \\ + \underbrace{\chi^\top P_c\chi + \frac{1}{2}||z||^2}_{V_{TC}}\,, \tag{53}$$

and let us start analysing

$$\dot{V}_{PF} = \sum_{i=1}^{n}\left(k_x e_{xi}^\top\dot{e}_{xi} + me_{vi}^\top\dot{e}_{vi} + \frac{1}{2}e_{\tilde{R}i}^\top\tilde{\omega}_i + c_1e_{vi}^\top\dot{e}_{xi} + c_1e_{xi}^\top\dot{e}_{vi}\right)$$

Next, consider

$$m\dot{e}_{vi} = m\frac{\partial^2 x_{di}}{\partial\gamma_i^2}z_i + m\frac{\partial^2 x_{di}}{\partial\gamma_i^2} + mg\vec{e}_3 - f_i\vec{b}_{3i}\,. \tag{54}$$

Adding and subtracting the term $\frac{f_i\vec{b}_{3di}}{\vec{b}_{3di}\cdot\vec{b}_{3i}}$ from the previous equation we get:

$$m\dot{e}_{vi} = m\frac{\partial^2 x_{di}}{\partial\gamma_i^2}z_i + m\frac{\partial^2 x_{di}}{\partial\gamma_i^2} + mg\vec{e}_3 - \frac{f_i\vec{b}_{3di}}{\vec{b}_{3di}^\top\vec{b}_{3i}} + \\ - \frac{f_i}{\vec{b}_{3di}^\top\vec{b}_{3i}}\left((\vec{b}_{3di}^\top\vec{b}_{3i})\vec{b}_{3i} - \vec{b}_{3di}\right) \tag{55}$$

Let $X_i = \frac{f_i}{\vec{b}_{3di}^\top\vec{b}_{3i}}\left((\vec{b}_{3di}^\top\vec{b}_{3i})\vec{b}_{3i} - \vec{b}_{3di}\right)$. Note that X_i is bounded as follow: [11]

$$||X_i|| \leq (k_x||e_{xi}|| + k_v||e_{vi}|| + B_i)||e_{\tilde{R}i}||\,. \tag{56}$$

Let also

$$A_i = -\left(k_x e_{xi} + k_v e_{vi} + mge_3 + m\frac{\partial^2 x_{di}}{\partial\gamma_i^2}\right)\,.$$

Then we note, from the definition of b_{3D} and $f_i(t)$ in (6) and (26), that $f_i = -A_i^\top\vec{b}_{3i}$, $\vec{b}_{3di} = -\frac{A_i}{||A_i||}$ and $-A_i = ||A_i||\vec{b}_{3di}$. Therefore

$$\frac{f_i\vec{b}_{3di}}{\vec{b}_{3di}^\top\vec{b}_{3i}} = \frac{(-A_i^\top\vec{b}_{3i})\vec{b}_{3di}}{\vec{b}_{3di}^\top\vec{b}_{3i}} = ||A_i||\vec{b}_{3di} = -A_i.$$

Then, equation (55) becomes:

$$m\dot{e}_{vi} = -k_x e_{xi} - k_v e_{vi} - X_i + m\frac{\partial^2 x_{di}}{\partial\gamma_i^2}z_i\,, \tag{57}$$

which allows us to rewrite:

$$\dot{V}_{PF} = \sum_{i=1}^{n}\left(k_x e_{xi}^\top\left(\frac{\partial x_{di}}{\partial\gamma_i}z_i + e_{vi}\right) + \right. \\ + e_{vi}^\top\left(-k_x e_{xi} - k_v e_{vi} - X_i + m\frac{\partial^2 x_{di}}{\partial\gamma_i^2}z_i\right) + \\ + \frac{1}{2}e_{\tilde{R}i}^\top\tilde{\omega}_i + c_1e_{vi}^\top\left(\frac{\partial x_{di}}{\partial\gamma_i}z_i + e_{vi}\right) + \\ \left. + \frac{c_1}{m}e_{xi}^\top\left(-k_x e_{xi} - k_v e_{vi} - X_i + m\frac{\partial^2 x_{di}}{\partial\gamma_i^2}z_i\right)\right)\,.$$

Substituting the control law for the angular velocity introduced in (27), and after straightforward computations, we have

$$\dot{V}_{PF} \leq \sum_{i=1}^{n}\left(-\frac{c_1k_x}{m}||e_{xi}||^2 - (k_v - c_1)||e_{vi}||^2 - k_{\tilde{R}i}||e_{\tilde{R}i}||^2 + \right. \\ + \frac{c_1k_v}{m}||e_{xi}||||e_{vi}|| + ||X_i||\left(\frac{c_1}{m}||e_{xi}|| + ||e_{vi}||\right) + \\ + z_i^\top\left((k_x\frac{\partial x_{di}}{\partial\gamma} + c_1\frac{\partial^2 x_{di}}{\partial\gamma^2})^\top e_{xi} + \right. \\ \left.\left. + (c_1\frac{\partial x_{di}}{\partial\gamma} + m\frac{\partial^2 x_{di}}{\partial\gamma^2})^\top e_{vi}\right)\right)\,.$$

Finally, using inequality (56) and the bound in (48), yields to:

$$\begin{aligned}\dot{V}_{PF} \leq & \sum_{i=1}^{n}\Bigg(-\frac{c_1 k_x}{m}(1-c^2)||e_{xi}||^2-(k_v(1-c^2)-c_1)||e_{vi}||^2+\\ & -k_{\tilde{R}i}||e_{\tilde{R}i}||^2+\frac{c_1 k_v}{m}(1+c^2)||e_{xi}||||e_{vi}||+\\ & +(k_x e_{x\max i}+B)||e_{\tilde{R}i}||||e_{vi}||+\frac{B_i c_1}{m}||e_{\tilde{R}i}||||e_{xi}||+\\ & +z_i^\top\Bigg((k_x\frac{\partial x_{di}}{\partial\gamma}+c_1\frac{\partial^2 x_{di}}{\partial\gamma^2})^\top e_{xi}+\\ & +(c_1\frac{\partial x_{di}}{\partial\gamma}+m\frac{\partial^2 x_{di}}{\partial\gamma^2})^\top e_{vi}\Bigg)\Bigg)\,.\end{aligned} \tag{58}$$

At this point note that, from the definition of e_x, e_v and $e_{\tilde{R}}$, the following hold:

$$\sum_{i=1}^{n}||e_{xi}||^2=||e_x||^2\,,\quad \sum_{i=1}^{n}||e_{vi}||^2=||e_v||^2\,,$$

$$\sum_{i=1}^{n}||e_{\tilde{R}i}||^2=||e_{\tilde{R}}||^2\,,$$

$$\sum_{i=1}^{n}||e_{xi}||||e_{vi}||\leq|||e_x||||e_v||\,,\quad \sum_{i=1}^{n}||e_{xi}||||e_{\tilde{R}i}||\leq|||e_x||||e_{\tilde{R}}||\,,$$

$$\sum_{i=1}^{n}||e_{\tilde{R}i}||||e_{vi}||\leq|||e_{\tilde{R}}||||e_v||\,.$$

Therefore, we get:

$$\begin{aligned}\dot{V}_{PF} \leq & -\frac{c_1 k_x}{m}(1-c^2)||e_x||^2-(k_v(1-c^2)-c_1)||e_v||^2+\\ & -k_{\tilde{R}}||e_{\tilde{R}}||^2+\frac{c_1 k_v}{m}(1+c^2)||e_x||||e_v||+\\ & +(k_x e_{x\max i}+B)||e_{\tilde{R}}||||e_v||+\frac{B_i c_1}{m}||e_{\tilde{R}}||||e_x||+\\ & +(k_x b_1+c_1 b_2)||z||||e_x||+(c_1 b_1+m b_2)||z||||e_v||\,.\end{aligned} \tag{59}$$

Now consider

$$\begin{aligned}\dot{V}_{TC} =&\chi^\top P_c\left(-\frac{a}{b}\bar{L}\chi+\frac{a}{b}QLz\right)+\left(-\frac{a}{b}\chi^\top\bar{L}+\frac{a}{b}z^\top LQ^\top\right)P_c\chi+\\ &+\chi^\top\dot{P}_c\chi+z^\top\left(-\left(bI-\frac{a}{b}L\right)z-\frac{a}{b}LQ^\top\chi\right)\end{aligned}$$

Letting $a\triangleq b$, we get:

$$\begin{aligned}\dot{V}_{TC} =&\chi^\top(\dot{P}_c-P_c\bar{L}-\bar{L}P_c)\chi-z^\top(bI-L)z+\chi^\top PQLz+\\ &+z^\top LQ^\top P\chi-z^\top LQ^\top\chi\,.\end{aligned}$$

Recalling the bounds of P_c in (43) and (44), and noting that $||Q||=1$ and $||L||\leq n$, we can write:

$$\dot{V}_{TC}\leq-\bar{c}_3||\chi||^2-(b-n)||z||^2+n\left(\frac{\bar{c}_4}{\gamma_\lambda}+1\right)||\chi||||z||\,. \tag{60}$$

We can finally now reconsider

$$\begin{aligned}\dot{V} =&\dot{V}_{PF}+\dot{V}_{TC}\\ \leq & -\frac{c_1 k_x}{m}(1-c^2)||e_x||^2-(k_v(1-c^2)-c_1)||e_v||^2+\\ & -k_{\tilde{R}}||e_{\tilde{R}}||^2+\frac{c_1 k_v}{m}(1+c^2)||e_x||||e_v||+\\ & +(k_x e_{x\max i}+B)||e_{\tilde{R}}||||e_v||+\frac{B_i c_1}{m}||e_{\tilde{R}}||||e_x||+\\ & +(k_x b_1+c_1 b_2)||z||||e_x||+(c_1 b_1+m b_2)||z||||e_v||+\\ & -\bar{c}_3||\chi||^2-(b-n)||z||^2+n\left(\frac{\bar{c}_4}{\gamma_\lambda}+1\right)||\chi||||z||\,.\end{aligned} \tag{61}$$

Using the Young's inequality, we get:

$$\dot{V}\leq-x_{PF}^\top Q_{PF}x_{PF}-x_{TC}^\top Q_{TC}x_{TC}\,,$$

where Q_{PF} and Q_{TC} are defined in (62) and (63).

Choosing proper values for the control gains and parameters that satisfy inequalities (30) and (31), we can write

$$\begin{aligned}\dot{V}(t)\leq&-\lambda\Bigg(\frac{k_x}{2}||e_x||^2+\frac{m}{2}||e_v||^2+\frac{1}{2-c^2}||e_{\tilde{R}}||+c_1(e_v^\top e_x)+\\ &+\chi^\top P_c\chi+\frac{1}{2}||z||^2\Bigg)\leq-\lambda V(t)\,,\end{aligned} \tag{64}$$

where

$$\lambda\triangleq\min(\lambda_{PF}\,,\,\lambda_{TC})$$

and λ_{PF} and λ_{TC} were defined in (33) and (34), respectively. Therefore, we have

$$V(t)\leq V(0)e^{-\lambda t}\,.$$

Recall the transformation in (49). Then,

$$\begin{aligned}\chi(t)^\top P\chi(t)+\frac{1}{2}||z(t)||^2=&(b\xi(t)+Qz(t))^\top P(b\xi(t)+Qz(t))+\\ &+\frac{1}{2}||z(t)||^2\,.\end{aligned}$$

Noting that

$$\begin{aligned}(b\xi(t)+Qz(t))^\top P(b\xi(t)+Qz(t))+\frac{1}{2}||z(t)||^2\geq&\frac{b^2\bar{c}_3}{2n}||\xi(t)||^2+\\ &+\frac{b\bar{c}_3}{n}\xi(t)^\top z(t)+\frac{1}{2}\left(\frac{\bar{c}_3}{n}+1\right)||z(t)||^2\,,\end{aligned}$$

and

$$\begin{aligned}(b\xi(0)+Qz(0))^\top P(b\xi(0)+Qz(0))+\frac{1}{2}||z(0)||^2\leq&\frac{b^2\bar{c}_4}{2\gamma_\lambda}||\xi(0)||^2+\\ &+\frac{b\bar{c}_4}{\gamma_\lambda}\xi(0)^\top z(0)+\frac{1}{2}\left(\frac{\bar{c}_4}{\gamma_\lambda}+1\right)||z(0)||^2\,,\end{aligned}$$

then the following bound holds:

$$\begin{aligned}&\Bigg(\frac{k_x}{2}||e_x(t)||^2+\frac{m}{2}||e_v(t)||^2+\frac{1}{2-c^2}||e_{\tilde{R}}(t)||+\\ &+c_1(e_v(t)^\top e_x(t))+\frac{b^2\bar{c}_3}{2n}||\xi(t)||^2+\frac{b\bar{c}_3}{n}\xi(t)^\top z(t)+\\ &+\frac{1}{2}\left(\frac{\bar{c}_3}{n}+1\right)||z(t)||^2\Bigg)\leq\Bigg(\frac{k_x}{2}||e_x(0)||^2+\frac{m}{2}||e_v(0)||^2+\\ &+\frac{1}{2-c^2}||e_{\tilde{R}}(0)||+c_1(e_v(0)^\top e_x(0))+\frac{b^2\bar{c}_4}{2\gamma_\lambda}||\xi(0)||^2+\\ &+\frac{b\bar{c}_4}{\gamma_\lambda}\xi(0)^\top z(0)+\frac{1}{2}\left(\frac{\bar{c}_4}{\gamma_\lambda}+1\right)||z(0)||^2\Bigg)e^{-\lambda t}\,,\end{aligned} \tag{65}$$

which completes the proof.

Proof of Remark 1 We first want to proof that the candidate Lyapunov function is positive definite. To do so, we need to prove that

$$\begin{bmatrix}\frac{k_x}{2} & \frac{c_1}{2} & 0\\ \frac{c_1}{2} & \frac{m}{2} & 0\\ 0 & 0 & \frac{1}{2}\end{bmatrix}>0\,,$$

which is verified choosing:

$$k_x>\frac{c_1^2}{m}\,.$$

$$Q_{PF} = \begin{bmatrix} \left(k_x\left(\frac{c_1}{m}(1-c^2)-b_1\right)-c_1b_2\right) & -\frac{c_1k_v}{m}(1+c^2) & -\frac{B_ic_1}{m} \\ -\frac{c_1k_v}{m}(1+c^2) & (k_v(1-c^2)-c_1-c_1b_1-mb_2) & -(k_xe_{x\max}+B) \\ -\frac{B_ic_1}{m} & -(k_xe_{x\max i}+B) & k_{\tilde{R}} \end{bmatrix} \tag{62}$$

$$Q_{TC} = \begin{bmatrix} \bar{c}_3 & -n\left(\frac{\bar{c}_4}{\gamma_\lambda}+1\right) \\ -n\left(\frac{\bar{c}_4}{\gamma_\lambda}+1\right) & (b-n-(k_x+c_1)b_1-(c_1+m)b_2) \end{bmatrix} \tag{63}$$

Then we want to proof that $\det(Q_{PF}-\lambda W_{12})\geq 0$, which is

$$\det(Q_{PF}-\lambda W_{12}) = \left(k_x\left(\frac{c_1}{m}(1-c^2)-b_1-\frac{\lambda_{PF}}{2}\right)-c_1b_2\right)$$
$$\left(k_v(1-c^2)-c_1-c_1b_1-mb_2-\lambda_{PF}\frac{m}{2}\right)\left(k_{\tilde{R}}-\lambda_{PF}\frac{1}{2-c^2}\right)+$$
$$-2(k_xe_{x\max}+B)\frac{Bc_1}{m}\left(\frac{c_1k_v}{m}(1+c^2)+\lambda_{PF}\frac{c_1}{2}\right)+$$
$$-\frac{B^2c_1^2}{m^2}\left(k_v(1-c^2)-c_1-c_1b_1-mb_2-\lambda_{PF}\frac{m}{2}\right)-$$
$$(k_xe_{x\max}+B)^2\left(k_x\left(\frac{c_1}{m}(1-c^2)-b_1-\frac{\lambda}{2}\right)-c_1b_2\right)+$$
$$-\left(k_{\tilde{R}}-\frac{\lambda_{PF}}{2-c^2}\right)\left(\frac{k_vc_1}{m}(1+c^2)+\lambda_{PF}\frac{c_1}{2}\right)^2\geq 0\,.$$

Choosing

$$k_x > \frac{c_1b_2+\left(\frac{k_vc_1}{m}(1+c^2)+\lambda_{PF}\frac{c_1}{2}\right)^2}{\frac{c_1}{m}(1-c^2)-b_1-\frac{\lambda}{2}}\,,$$

$$c_1 > \frac{m\left(b_1+\frac{\lambda_{PF}}{2}\right)}{1-c^2}$$

and

$$k_v > \frac{c_1+c_1b_1+mb_2+\frac{m}{2}\lambda_{PF}+2}{1-c^2}$$

we have:

$$\det(Q_{PF}-\lambda_{PF}W_{12}) > \left(k_{\tilde{R}}-\frac{\lambda_{PF}}{2-c^2}\right)$$
$$\cdot\left(\frac{k_vc_1}{m}(1+c^2)+\lambda_{PF}\frac{c_1}{2}\right)^2+$$
$$-2(k_xe_{x\max}+B)\frac{Bc_1}{m}\left(\frac{c_1k_v}{m}(1+c^2)+\lambda_{PF}\frac{c_1}{2}\right)+$$
$$-\frac{B^2c_1^2}{m^2}(k_v(1-c^2))-(k_xe_{x\max}+B)^2\left(k_x\left(\frac{c_1}{m}(1-c^2)\right)\right)\,.$$

Finally, if $k_{\tilde{R}}$ satisfies (66), then $\det(Q_{PF}-\lambda_{PF}W_{12})\geq 0$ for any $\lambda_{PF}>0$.

At last, we need to prove inequality (31). Remembering that

$$\gamma_\lambda \geq \bar{\gamma}_\lambda \triangleq \frac{\mu}{T(1+n^2T)^2}\,,$$

and choosing $\bar{c}_3=\bar{c}_4$ and $\lambda_{TC}<\frac{\mu}{T(1+n^2T)^2}$, we get

$$\begin{bmatrix} \frac{\bar{c}_3}{2} & -n\left(\frac{\bar{c}_4}{\gamma_\lambda}+1\right) \\ -n\left(\frac{\bar{c}_4}{\gamma_\lambda}+1\right) & (b-n-(k_x+c_1)b_1-(c_1+m)b_2-\frac{\lambda_{TC}}{2}) \end{bmatrix}\geq 0\,,$$

which is verified choosing

$$b > n+(k_x+c_1)b_1+(c_1+m)b_2+\frac{\lambda_{TC}}{2}+\frac{2n^2}{\bar{c}_3}\left(\frac{\bar{c}_4}{\gamma_\lambda}+1\right)^2\,. \tag{67}$$

Proof of Lemma 2 Consider the Lyapunov function introduced in Appendix (see (52)). Adding and subtracting the term $f_{ci}\vec{b}_{3i}$ from (54) leads to

$$m\dot{e}_{vi} = m\frac{\partial^2 x_{di}}{\partial\gamma_i^2}z_i + m\frac{\partial^2 x_{di}}{\partial\gamma_i^2} + mg\vec{e}_3 - f_{ci}\vec{b}_{3i} + [f_{ci}-f_i]\vec{b}_{3i}\,.$$

Following the same argument used before, we get:

$$m\dot{e}_{vi} = -k_xe_{xi}-k_ve_{vi}-X_i+m\frac{\partial^2 x_{di}}{\partial\gamma_i^2}z_i+[f_{ci}-f_i]\vec{b}_{3i}\,.$$

Therefore, we can write:

$$\dot{V}_{PF} = \sum_{i=1}^{n}\left(k_xe_{xi}^\top\left(\frac{\partial x_{di}}{\partial\gamma_i}z_i+e_{vi}\right)+e_{vi}^\top(-k_xe_{xi}-k_ve_{vi}+\right.$$
$$-X_i+m\frac{\partial^2 x_{di}}{\partial\gamma_i^2}z_i+[f_{ci}-f_i]\vec{b}_{3i}\Big)+$$
$$\frac{1}{2}e_{\tilde{R}i}^\top\left(\begin{bmatrix}p_i\\q_i\\r_i\end{bmatrix}-\tilde{R}_i^\top\omega_{D_iI}^{D_i}\right)+c_1e_{vi}^\top\left(\frac{\partial x_{di}}{\partial\gamma_i}z_i+e_{vi}\right)+$$
$$\frac{c_1}{m}e_{xi}^\top\left(-k_xe_{xi}-k_ve_{vi}-X_i+m\frac{\partial^2 x_{di}}{\partial\gamma_i^2}z_i+\right.$$
$$\left.\left.+[f_{ci}-f_i]\vec{b}_{3i}\right)\right)\,.$$

Then, adding and subtracting the term $\sum_{i=1}^n\frac{1}{2}e_{\tilde{R}i}\begin{bmatrix}p_{ci}\\q_{ci}\\r_{ci}\end{bmatrix}$, and recalling the result obtained in before in this Appendix (see (64)) we get:

$$\dot{V}(t)\leq-\lambda\left(\frac{k_x}{2}||e_x||^2+\frac{m}{2}||e_v||^2+\frac{1}{2-c^2}||e_{\tilde{R}}||^2+c_1(e_v^\top e_x)+\right.$$
$$\left.\chi^\top P_c\chi+\frac{1}{2}||z||^2\right)+\frac{c_1}{m}\delta_f||e_x||+\delta_f||e_v||+\frac{1}{2}\delta_\omega||e_{\tilde{R}}||\,,$$

which can also be written as:

$$\dot{V}(t)\leq-(\lambda-\theta)\left(\frac{k_x}{2}||e_x||^2+\frac{m}{2}||e_v||^2+\frac{1}{2-c^2}||e_{\tilde{R}}||^2+\right.$$
$$\left.+c_1(e_v^\top e_x)+\chi^\top P_c\chi+\frac{1}{2}||z||^2\right)-\theta\left(\frac{k_x}{2}||e_x||^2+\right.$$
$$+\frac{m}{2}||e_v||^2+\frac{1}{2-c^2}||e_{\tilde{R}}||^2+c_1(e_v^\top e_x)+$$
$$\left.+\chi^\top P_c\chi+\frac{1}{2}||z||^2\right)+\frac{c_1}{m}\delta_f||e_x||+\delta_f||e_v||+$$
$$+\frac{1}{2}\delta_\omega||e_{\tilde{R}}||\,,$$

where $0<\theta<\lambda$. Then, for all the $x=[e_x^\top\,,e_v^\top\,,e_{\tilde{R}}^\top\,,\xi^\top\,,z^\top]^\top$

$$k_{\tilde{R}} \geq \frac{2(k_x e_{x\max}+B)\frac{Bc_1}{m}\left(\frac{c_1 k_v}{m}(1+c^2)+\lambda_{PF}\frac{c_1}{2}\right)+\frac{B^2c_1^2}{m^2}(k_v(1-c^2))+(k_x e_{x\max}+B)^2\left(k_x\left(\frac{c_1}{m}(1-c^2)\right)\right)}{\left(\frac{k_v c_1}{m}(1+c^2)+\lambda_{PF}\frac{c_1}{2}\right)^2}+\frac{\lambda_{PF}}{2-c^2} \tag{66}$$

satisfying

$$-\theta\left(\frac{k_x}{2}||e_x||^2+\frac{m}{2}||e_v||^2+\frac{1}{2-c^2}||e_{\tilde{R}}||^2+c_1(e_v^\top e_x)+\right.$$
$$\left.+\chi^\top P_c\chi+\frac{1}{2}||z||^2\right)+\frac{c_1}{m}\delta_f||e_x||+\delta_f||e_v||+\frac{1}{2}\delta_\omega||e_{\tilde{R}}||\leq 0\,, \tag{68}$$

we have

$$\dot{V}_{PF}(t)\leq-(\lambda-\theta)V(t)\,.$$

Note that (68) can be written as

$$-\theta\left(\frac{k_x}{2}||e_x||^2\left(1-\frac{2c_1}{k_x m}\frac{\delta_f}{\theta}\frac{1}{||e_x||}\right)+\frac{m}{2}||e_v||^2\left(1-\frac{2\delta_f}{m\theta}\frac{1}{||e_v||}\right)\right.$$
$$+\frac{1}{2-c^2}||e_{\tilde{R}}||^2\left(1-\frac{2-c^2}{2}\frac{\delta_\omega}{\theta}\frac{1}{||e_{\tilde{R}}||}\right)+c_1(e_v^\top e_x)+$$
$$\left.+\chi^\top P_c\chi+\frac{1}{2}||z||^2\right)\leq 0\,.$$

We note that, outside the bounded set

$$\Omega_d\triangleq\left\{x=[e_x^\top\,,e_v^\top\,,e_{\tilde{R}}^\top\,,\chi^\top\,,z^\top]^\top\ \text{ s.t.}\right.$$
$$||e_x||\leq\frac{2c_1\delta_f}{k_x m\theta(1-\epsilon_x)}\,,\ ||e_v||\leq\frac{2\delta_f}{m\theta(1-\epsilon_v)}\,,$$
$$\left.||e_{\tilde{R}}||\leq\frac{2-c^2}{2}\frac{\delta_\omega}{\theta}\right\}\,,$$

with $0<\epsilon_x<1$ and $0<\epsilon_v<1$, inequality (68) is satisfied by choosing

$$k_x\geq\frac{4c_1^2}{m\epsilon_x\epsilon_v}\,.$$

Moreover, if the performance bounds satisfy the following constrains:

$$\delta_f<\frac{e_{x\max}k_x m\theta}{2c_1}\,,$$
$$\delta_\omega<\frac{2\theta c^2}{2-c^2}\,,$$

then $\Omega_d\subset\Omega_c$ defined in (35). With the above result, it can be shown that, for every initial state $x=[e_x(0)\,,e_v(0)\,,e_{\tilde{R}}(0)\,,\xi(0)\,,z(0)]\in\Omega_c$, there is a time $T_b\geq 0$ such that the bound in (39) is satisfied $\forall\ 0\leq t<T_b$, and the bound in (40) is satisfied $\forall\ t\geq T_b$.

Proof of Remark 2 In Lemma 2 was discussed the convergence of the path following and time coordination errors in presence of limited performance of the autopilot. Even though the limits of the inner loop architecture affect the performance of the path following errors, we can prove that the time coordination keep converging to zero with rate of convergence λ_{TC}. In fact, recalling the definition of V_{TC} in Appendix and choosing the control law that solves the time coordinated 3D path following problem, we have (see (60)) :

$$\dot{V}_{TC}\leq-\bar{c}_3||\chi||^2-(b-n)||z||^2+n\left(\frac{\bar{c}_4}{\gamma_\lambda}+1\right)||\chi||||z||\,.$$

Then, with the same control gains discussed before, we get

$$\dot{V}_{TC}\leq-\lambda_{TC}V_{TC}\,.$$

Therefore

$$\left(\frac{b^2\bar{c}_3}{2n}||\xi(t)||^2+\frac{b\bar{c}_3}{n}\xi(t)^\top z(t)+\frac{1}{2}\left(\frac{\bar{c}_3}{n}+1\right)||z(t)||^2\right)$$
$$\leq\left(\frac{b^2\bar{c}_4}{2\gamma_\lambda}||\xi(0)||^2+\frac{b\bar{c}_4}{\gamma_\lambda}\xi(0)^\top z(0)+\right. \tag{69}$$
$$\left.+\frac{1}{2}\left(\frac{\bar{c}_4}{\gamma_\lambda}+1\right)||z(0)||^2\right)e^{-\lambda_{TC}t}\,,$$

holds $\forall\, t\geq 0$.